

A-Tract Polarity Dominate the Curvature in Flanking Sequences<sup>†</sup>

Ayelet Merling, Nataliya Sagaydakova, and Tali E. Haran\*

Department of Biology, Technion, Technion City, Haifa 32000, Israel

Received November 18, 2002; Revised Manuscript Received March 3, 2003

**ABSTRACT:** It is well-known, but little understood, that the nucleotide sequences between phased A<sub>4</sub>–A<sub>6</sub>-tracts (at 10–11 bp intervals) have only a slight effect on overall curvature. To explore this phenomenon, we have examined the gel-migration properties of sequences containing both A-tracts as well as G-tracts (i.e., sequences of the form G<sub>n</sub>C<sub>m</sub> or C<sub>n</sub>G<sub>m</sub>,  $n + m > 4$ ) in various relative positioning. We show that the composite bend of these sequences depends on their relative arrangement. When G-tracts are placed between two A-tracts, such that both tracts are repeated in phase to themselves (e.g., G<sub>5</sub>A<sub>6</sub>G<sub>5</sub>A<sub>5</sub>), or adjacent to the 3'-side of A-tracts (e.g., A<sub>6</sub>G<sub>5</sub>N<sub>10</sub>), they have minimal influence on the extent of bending of the composite sequence. When G-tracts are placed one helical repeat away from A-tracts (e.g., G<sub>5</sub>N<sub>5</sub>A<sub>6</sub>N<sub>6</sub>), or are adjacent only to the 5'-side of A-tracts (e.g., G<sub>5</sub>A<sub>6</sub>N<sub>10</sub>) their influence on the composite bend is larger. The differential behavior of AG- versus GA-tracts means that A-tracts influence their flanking sequences in a polar manner. Whereas they suppress, or make constant, the intrinsic bending characteristics of any sequence placed immediately 3' to them (and hence by definition any sequence placed between two phased A-tracts), sequences adjoining them on their 5'-side are free to modulate the overall curvature. We interpret these results as evidence for the dominant nature of the unique and nonuniform structure adopted by tracts of four adenines or more. The effects of A-tracts extend at least five base pairs into the adjoining 3' region. This is further evidence for the complexity of DNA structure and the inadequacy of simple nearest-neighbor models to explain all its manifestations.

The conformation and conformability of the DNA double helix are sequence dependent and are active participants in DNA recognition by drugs and proteins (reviewed in refs 1–3). A particular aspect of sequence-dependent DNA structure is that of sequence-dependent DNA bending, observed when the sequence contains phased repeats of A<sub>4</sub>–A<sub>6</sub>-tracts (A-tracts, reviewed in refs 4 and 5). The phenomenon of intrinsic DNA bending was discovered two decades ago, when restriction fragments from the kinetoplast body of *Leishmania tarentolae* appeared to migrate anomalously slow on polyacrylamide gels (PAG, ref 6). However, 20 years after the first observation of global intrinsic DNA bending (6) and its relationship to DNA sequences containing phased A-tracts (7), the phenomenon is still not completely understood. In particular, it is still debated where the locus (or loci) of bending is—entirely within A-tracts, entirely outside the A-tract region, or spread throughout the whole region in some relative proportion. Also debated are the molecular details of A-tract structure and whether A-tracts influence the structure of the sequences flanking them, or are being influenced by them.

Over the years several more DNA sequences have been shown to cause the DNA helix to deflect from being overall straight, as in the canonical Watson–Crick model, but none shows a phenomenon as large as that of phased A<sub>4</sub>–A<sub>6</sub>-tracts. Among the dinucleotides the C–A step is notable (8–10). Among the longer tracts GGGCCC has been extensively

studied. GGGCCC has been shown to be slightly bent toward the major groove (11, 12). Bending by GGGCCC was shown to be significantly increased in the presence of Mg<sup>2+</sup> ions (12–14). The major-groove direction of bending is preserved in the presence of Mg<sup>2+</sup> ions (13, 28). Mg<sup>2+</sup> ions were shown to induce curvature in the CCCGGG element as well, with the bending being in opposite direction to that in GGGCCC (28). The direction of bending, of the GGGCCC and the CCCGGG elements, which were deduced from DNaseI digestion studies and helical phasing experiments, are opposite to those predicted from dinucleotide models (16, 17) as well as those observed for the G–C and the C–G steps, respectively, in crystalline structures (analyzed in ref 18). This underscores the complexity of DNA structure, which may not always yield to simple nearest-neighbor analysis. GGGGGG was also shown to cause slight curvature when properly phased (19).

We have constructed a series of molecules containing various combinations of G,C-rich sequence motifs of the general form G<sub>n</sub>C<sub>m</sub> or C<sub>n</sub>G<sub>m</sub> ( $n + m > 4$ , collectively called G-tracts) and A-tracts (Table 1) and have looked at their gel-electrophoretic migration pattern. We use these sequences to examine the inter-relationship of G- and A-tracts in various sequence settings. We have chosen to use G-tracts for this purpose because each of these tracts apparently acts as a single unit, in which the structure is cooperatively built by a whole pentamer or hexamer. Our findings demonstrate the nonuniformity of A-tract structure and its differential effect on sequences placed at the 3' versus the 5' side of A-tracts. Furthermore, we show that the effect of A-tracts on its

<sup>†</sup> This work was supported by the Israel Science Foundation (T.E.H.).

\* Corresponding author. Phone: 972-4-8293767. Fax: 972-4-8225153. E-mail: bitali@tx.technion.ac.il.

Table 1: Oligodeoxynucleotides Used in This Study<sup>a</sup>

name	sequence	$R_L$ (147)	curvature (deg)
Class: G-tracts in phase with themselves			
CG	5' <u>CCCCGGT</u> CGCT <u>CCCCGGT</u> ACGT		
GC	5' <u>GGGCCCT</u> CGCT <u>GGGCCCT</u> ACGT		
GG	5' <u>GGGGGGT</u> CGCT <u>GGGGGGT</u> ACGT		
Class II: G-tracts half a repeat away from A-tracts			
CGAA	5' <u>CCCCG</u> <b>AAAAAC</b> <u>CCCG</u> <b>AAAAAA</b>	2.62	17.8(2)
GCAA	5' <u>GGGCC</u> <b>AAAAAG</b> <u>GGCC</u> <b>AAAAAA</b>	2.71	18.3(3)
GGAA	5' <u>GGGGG</u> <b>AAAAAG</b> <u>GGGG</u> <b>AAAAAA</b>	2.71	18.3(3)
Class III: G-tracts 1 repeat away from A-tracts			
CGPAA	5' <u>CCCCG</u> TCGCT <b>AAAAA</b> TACGT	1.38	9.0(1)
GCPAA	5' <u>GGGCC</u> TCGCT <b>AAAAA</b> TACGT	1.20	6.7(2)
GGPAA	5' <u>GGGGG</u> TCGCT <b>AAAAA</b> TACGT	1.26	7.4(2)
Class IV: Double motifs			
DAADCG	5' <b>AAAAA</b> TTCGCT <b>AAAAA</b> TACGT <u>CCCCGGT</u> CGCT <u>CCCCGGT</u> ACGT	1.45	9.3(2)
DAADGC	5' <b>AAAAA</b> TTCGCT <b>AAAAA</b> TACGT <u>GGGCCCT</u> CGCT <u>GGGCCCT</u> ACGT	1.24	6.96(4)
DAADGG	5' <b>AAAAA</b> TTCGCT <b>AAAAA</b> TACGT <u>GGGGGGT</u> CGCT <u>GGGGGGT</u> ACGT	1.26	6.9(2)
Class V: 3' A/G blocks			
ACGBL	5' <b>AAAAAA</b> <u>CCCCGGT</u> ACGTTTCGCT	1.35	8.44(6)
AGCBL	5' <b>AAAAAA</b> <u>GGGCCCT</u> ACGTTTCGCT	1.35	8.42(6)
AGGBL	5' <b>AAAAAA</b> <u>GGGGGT</u> ACGTTTCGCT	1.37	8.8(2)
Class VI: 5' A/G blocks			
CGABL	5' <u>CCCCG</u> <b>AAAAA</b> TACGTTTCGCT	1.20	6.47(3)
GCABL	5' <u>GGGCC</u> <b>AAAAA</b> TACGTTTCGCT	1.43	9.35(6)
GGABL	5' <u>GGGGG</u> <b>AAAAA</b> TACGTTTCGCT	1.37	8.66(4)
Class VII: Bend magnitude calibrators			
A <sub>6</sub> A <sub>5</sub> neut	5'TCGCT <b>AAAAA</b> TACGT <b>AAAAAA</b>	2.73	18.4(2)
A <sub>6</sub> neut	5'CGCGCTACGT <b>AAAAA</b> TTCGCT	1.36	8.52(3)
Size markers			
VW	5'TCGGATCCGTCGACCATCTGT		
str. cont.	5'TCGCTCGCGCTACGTCGCGCG		

<sup>a</sup> Only one strand of each duplex is shown. All duplexes were produced with 2-bp 5'-overhanging ends, except for A<sub>6</sub>neut, which has 3-bp protruding 5' ends. The  $R_L$  values, at chain length 147 bp, are from Figure 1, and they correspond to one gel out of three to six independent experiments. Curvature values were calculated relative to the sequence A<sub>6</sub>I/1 ( $18 \pm 2^\circ$ , see Materials and Methods and ref 25) and were calculated by the equation of Koo and Crothers (24). They are the average of three to six independent experiments. The number in parentheses are the standard error of the mean. A-tracts are in bold, and the G-tracts are in underlined italics.

flanking sequences extends at least five base pairs downstream from the last A in the tract. The influence of A-tracts on these sequences suppressed their intrinsic structure and curvature.

## MATERIALS AND METHODS

The oligodeoxynucleotides of Tables 1 and 2 were synthesized on an automated DNA synthesizer. The deprotected oligodeoxynucleotides were purified on denaturing PAG using standard procedures (20). Each single-stranded oligodeoxynucleotide (3  $\mu$ g) was 5'-end labeled with 4  $\mu$ Ci of [ $\gamma$ -<sup>32</sup>P]ATP (sp. act. >6000 Ci/mmol) and 3 units of T4 polynucleotide kinase (New England Biolabs) in a 14  $\mu$ L solution for 30 min at 37 °C. This was followed by the addition of 1 mM cold ATP and 3 more units of T4 polynucleotide kinase for an additional 30 min at 37 °C. Complementary oligodeoxynucleotides were hybridized by heating to 95 °C and cooling the solution overnight. The hybridized oligodeoxynucleotides were multimerized by the addition of 4 units of T4 DNA ligase to 60% of each of the hybridized molecules and incubation at 16 °C overnight. This was followed by the addition of the remaining 40% of each of the hybridized molecules and an additional 4 units of T4 DNA ligase for 20 min at room temperature. This ensures that the ligation ladders contain both high as well as low molecular weight fragments. The reaction was stopped by

the addition of 30 mM EDTA,<sup>1</sup> followed by purification of the products on G-25 spin columns equilibrated with TE buffer (10 mM Tris-HCl, pH 8.0, 1 mM EDTA). To separate the various multimers of the oligodeoxynucleotides, the products of the ligation reactions were electrophoresed on a native 8% (acrylamide/bisacrylamide ratio 29:1) gel in 0.09 M Tris-borate, 2 mM EDTA buffer at 20 °C in a Hoffer thermostated gel box. The gels were run at 300 V until the BPB dye migrated 24 cm in a 20 cm  $\times$  32 cm  $\times$  0.75 mm gel. Three to six independent experiments were carried out. In each experiment, the location of each class of sequences on the gel was varied, so that the position on the gel (center vs the edges of the gel) will not systematically bias the experimental results.

The ratio of apparent length to real chain length (both in base-pairs),  $R_L$ , was calculated relative to a random B-DNA size marker, VW (Table 1), used in our previous studies (21–23). Curvature was calculated by the equation of Koo and Crothers (24) relative to the curvature of A<sub>6</sub>I/1 (GGGCAA-AAAACGGCAAAAAAC), which is  $18 \pm 2^\circ$  (25).

## RESULTS AND DISCUSSION

*DNA Bending of G-Tracts Depend on Their Positioning Relative to A-Tracts.* Each oligonucleotide in Table 1

<sup>1</sup> Abbreviations: bp, base pairs; EDTA, *N,N,N',N'*-ethylenediaminetetraacetic acid; BPB, Bromophenol Blue.

Table 2: A- and G-Tracts in Various Sequence Repeats<sup>a</sup>

name	sequence	app. helix twist	$R_L$ (150) max.	curvature (deg)
Class I: G-tracts in phase with themselves				
CG21	5' <u>CCCGGG</u> TCGCT <u>CCCGG</u> TACGT		1.11	
CG22	5' <u>CCCGGG</u> TCGCT <u>CCCGG</u> TACGT			
CG23	5' <u>CCCGGG</u> TCGCT <u>CCCGG</u> TACGT			
GG21	5' <u>GGGGGG</u> TCGCT <u>GGGGG</u> TACGT		1.22	
GG22	5' <u>GGGGGG</u> TCGCT <u>GGGGG</u> TACGT	11.08(2)		
GG23	5' <u>GGGGGG</u> TCGCT <u>GGGGG</u> TACGT			6.5(4)
GC21	5' <u>GGGCC</u> TCGCT <u>GGGCC</u> TACGT		1.66	
GG22	5' <u>GGGCC</u> TCGCT <u>GGGCC</u> TACGT	11.18(1)		
GC23	5' <u>GGGCC</u> TCGCT <u>GGGCC</u> TACGT			11.20(2)
GC32	5' <u>GGGCC</u> TCGCT <u>GGGCC</u> TACGT <u>GGGCC</u> TGTCT			
Class III: G-tracts 1 repeat away from A-tracts				
CGPAA20	5' <u>CCCGG</u> TCGCT <u>AAAAA</u> TACGT		1.41	
CGPAA21	5' <u>CCCGG</u> TCGCT <u>AAAAA</u> TACGT	10.45		
CGPAA22	5' <u>CCCGG</u> TCGCT <u>AAAAA</u> TACGT			8.9(2)
GGPAA20	5' <u>GGGGG</u> TCGCT <u>AAAAA</u> TACGT		1.30	
GGPAA21	5' <u>GGGGG</u> TCGCT <u>AAAAA</u> TACGT	10.28(1)		
GGPAA22	5' <u>GGGGG</u> TCGCT <u>AAAAA</u> TACGT			7.0(2)
GCPAA20	5' <u>GGGCC</u> TCGCT <u>AAAAA</u> TACGT		1.26	
GCPAA21	5' <u>GGGCC</u> TCGCT <u>AAAAA</u> TACGT	10.36(2)		
GCPAA22	5' <u>GGGCC</u> TCGCT <u>AAAAA</u> TACGT			6.8(3)
Size marker				
A <sub>6</sub> neut20	5'CGCGCTACGT <u>AAAAA</u> TCGCT		1.39	
A <sub>6</sub> neut21	5'CGCGCTACGT <u>AAAAA</u> TCGCT	10.29(3)		
A <sub>6</sub> neut22	5'GCGCGCTACGT <u>AAAAA</u> TCGCT			8.59(2)

<sup>a</sup> Only one strand of each duplex is shown. All duplexes were produced with 2-bp 5'-overhanging ends, except for A<sub>6</sub>neut, which has 3-bp protruding 5' ends. The  $R_L$  values, at chain length 150 bp, are from Figures 2 and 3, and they correspond to one gel out of three to six independent experiments. Curvature values were calculated relative to the sequence A<sub>6</sub>I/1 ( $18 \pm 2^\circ$ , see Materials and Methods and ref 25) and were calculated by the equation of Koo and Crothers (24). They are the average of three to six independent experiments. The number in parentheses are the standard error of the mean. A-tracts are in bold, and the G-tracts are in underlined italics.

contains one type of G-tract, which is either repeated in phase with itself (class I); or is between two phased A-tracts (class II), such that both the A-tracts as well as the G-tracts are repeated in phase to themselves but are one-half a repeat away from each other; or is one helical repeat away from an A-tract (classes III and IV); or is adjacent to one side of an A-tract only (classes V and VI). Initially, we synthesized the oligonucleotides (Table 1) as 21-bp-long fragments, so that in the multimers of the ligation ladders the various bending motifs will be separated from each other by an integral multiple of the helical repeat of random-sequence B-DNA in solution (10.5 bp/turn, refs 26 and 27); therefore, they will add up constructively.

To ensure that the overall bending of the double helix is due either to a G-tract or to an A-tract we have used five base-pair buffer sequences, which according to current knowledge are not by themselves significantly bent or bendable (15, 17, 28). These two pentamers are TCGCT and TACGT. When these two pentamers were placed one helical repeat apart from each other and separated by CGCGC and CGCGC (str. cont., Table 1) they migrated normally on PAG, relative to the size marker (VW, Table 1) used in all our previous studies (21–23, data not shown). Also included in Table 1 are two bend magnitude calibrators, A<sub>6</sub>A<sub>5</sub>neut and A<sub>6</sub>neut. They correspond to previous bend magnitude calibrators of one A-tract unit per helical repeat ( $18 \pm 2^\circ$ , refs 24 and 25) and one A-tract unit per two helical repeats ( $9 \pm 1^\circ$ , refs 24 and 25), respectively, but have the neutral pentamers separating the A- or G-tract motifs. Thus, we can compare the bending properties of the composite A- and

G-tracts sequences with sequences containing only A-tract sequences (A<sub>6</sub>neut for class II and A<sub>6</sub>A<sub>5</sub>neut for class III–VI sequences) to infer the net influence of the G-tract motifs on the composite bending.

We first compared the migration behavior on PAG of multimers of class I, G-tracts phased to themselves. Figure 1A shows that 21-bp multimers of G-tracts-only sequences do not show any significant anomaly in their migration on PAG, as previously observed (refs 12 and 14, but see below). When placed between two A-tracts (class II, Table 1), the migration anomaly in the gel is the same for all three G-tracts and is similar to the A-tract construct with the neutral spacer, A<sub>6</sub>A<sub>5</sub>neut (Figure 1B). This agrees with our previous study that showed that changing the sequences flanking A-tracts modulates the overall bending by only  $\pm 10\%$  (22). However, when the G- and the A-tract motifs are placed one helical repeat from each other, separated by a neutral pentamer (class III, Table 1), the three different sequences of this group show a more variable migration behavior on PAG, indicating greater modulation of A<sub>6</sub>-tract bending in these sequences, even though the G-tracts are now further away from the A-tracts (Figure 1C). The CCCGG motif seems to enhance the bending shown by a neutral A<sub>6</sub>-tract alone, as it migrates more slowly on PAG (as evidenced by the increase in the  $R_L$  value relative to A<sub>6</sub>neut). Since it is in phase with the A<sub>6</sub>-tract, it seems to bend in the same direction as this motif, namely, in the direction compressing the minor groove at the center of the sequence motif (reviewed in refs 4 and 5). GGGCC and GGGGG bend in the opposite direction to CCCGG and AAAAA because their  $R_L$  value is reduced

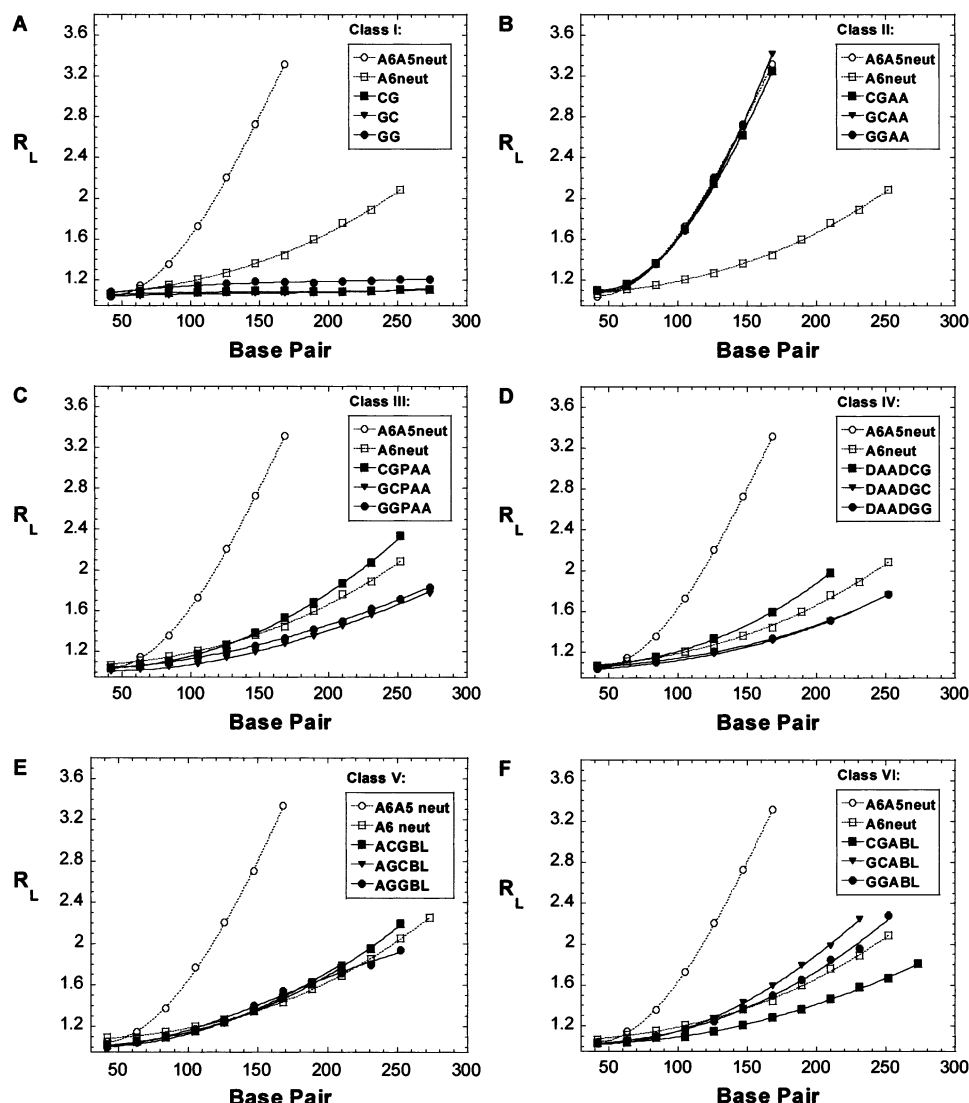


FIGURE 1:  $R_L$  values as a function of actual chain length (in bp) for multimers of sequences with monomeric length of 21 bp (Table 1).  $R_L$  is the ratio of apparent length (in bp), determined from comparison with a size marker sequence, to real chain length (in bp). Each plot contains the graphs of one class of sequences (I–VI) plus bend magnitude calibrators (VII, Table 1). The results correspond to one of three to six independent experiments.

relative to that of  $A_6neut$  (i.e., they compress the major groove, as observed previously for GGGCC (13, 29)). Alternatively, it may well be that the CCCGGG containing sequences are the true  $A_6neut$ , in the sense that these sequences represent the net bending of an  $A_6$ -tract and that the CCCGGG motif does not contribute significantly to the combined A + G-tract bending (see below). This possibility, however, does not affect the conclusion that GGGGGG- and GGGCCC-tracts are bent toward the major groove. Any sequence element that decrease the migration anomaly on PAG of A-tract containing sequences (and hence the  $R_L$  values) has to have an associated curvature pointing into the major groove at the center of the sequence, if the sequence elements are in phase with an A-tract (as they are in the PAA series, class III, Table 1). The extent of bending modulation is  $\pm 20\%$  at most (i.e., 40% difference between the curvature of the GGGCC and CCCGG containing sequences, Table 1) and not  $\pm 100\%$ , as proposed previously (29). This point is further discussed below.

To corroborate these results, we used DNA sequences containing an equal density of A- and G-tracts (class IV,

Table 1). Here, we have a double motif of each kind—one pentamer and one hexamer of A- and of G-tract, with 10.5 base pairs between each motif. Figure 1D shows that here too the range of the effect is around 40% between its extremes. Moreover, to ensure that no significant influence of G-tracts on A-tract bending goes undetected because of differences between the helical repeat and sequence repeat of these constructs, we repeated the experiment using sequences of class III (the PAA series of Table 1) with monomeric units 20-, 21-, and 22-bp long (Table 2). The results (Figure 2, Table 2) show that the apparent helical repeat of these sequences is close to 10.5 bp/turn, that the curvature at the maximum of each graph is within the experimental error of the results from the 21-bp set, and that the difference between the curvature at the maximum of the CGPAA versus the GCPAA graph is again 40% at most (i.e.,  $\pm 20\%$  around an averaged  $A_6$ -containing sequence).

*Polarity in the Influence of A-Tracts on Flanking Sequences.* Our observation (Figure 1B and ref 22) that any 5 bp sequence positioned between two A-tracts shows the same migration behavior on PAG, regardless of its particular

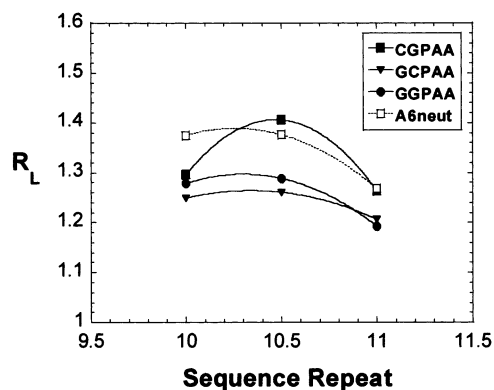


FIGURE 2:  $R_L$  values as a function of sequence repeat for multimers of chain length 150 bp for sequences of class III having a sequence repeat of 20–22 bp (Table 2). A bend magnitude calibrator ( $A_6$ -neut) with sequence repeat 20–22 bp is included for comparison. The maximum of the graphs represents the apparent helical twist of that sequence, and the  $R_L$  value at that point represents the twist-independent curvature of the sequence.

nature, suggests that these sequences do not express their true nature, the one shown when they are removed from the A-tract blocks (compare Figure 1B to C). It has been previously suggested that A-tract structure is not uniform but changes gradually from its 5' to its 3' end. In particular, it has been observed that the minor groove at the 5'-end is wide, whereas that in the 3'-end is narrower (30–32). To assess the degree of nonuniformity of A-tract structure and establish which end of the A-tract is responsible for the suppression of the true nature of the non-A-tract sequences positioned between them, we have constructed two more groups of DNA sequences containing a combination of A + G-tracts (classes V and VI in Table 1). In these two groups, the G-tracts are adjacent only to one side of the A-tract, either the 3'-side (Figure 1E) or the 5'-side (Figure 1F). These sequences have one  $A_6$  motif per two helical repeats and so should be compared in gel mobility to  $A_6$ -neut. Figure 1E shows that in all sequences with a G-tract adjacent to the 3' end of an A-tract the gel mobilities are indistinguishable from each other, as we observe for class II sequences (Figure 1B). However, when the various G-tracts are placed on the 5' side of an A-tract (Figure 1F), we see the reverse of the pattern of gel mobility observed in the PAA series (class III in Table 1). The difference between the extreme of bend modulation in Figure 1F is 46%, which is the largest difference observed between two sequences containing A-tracts.

**Extent of Bending by G-Tracts.** It is well-known that mixed sequence B-DNA molecules have a helical repeat around 10.5 bp/turn (26, 27). The helical repeat of sequences containing  $A_6$ -tracts is 10.34 bp/turn (33). However, G,C-rich sequences usually have a helical repeat around 11 bp/turn (19, 34). Hence, our analysis of the migration on PAG of the sequences listed in Table 1 is valid for all the studied sequences, as shown above for the PAA group (class III), except for class I sequences, which are G,C-rich sequences. To ensure that no bending phenomenon goes undetected in the G-tract-only sequences, we repeated the study of these sequences using ligation ladders with monomeric units 21-, 22-, and 23-bp long (Table 2). For the GGGCCC motif, we used a 32-bp monomeric unit as well because it has been

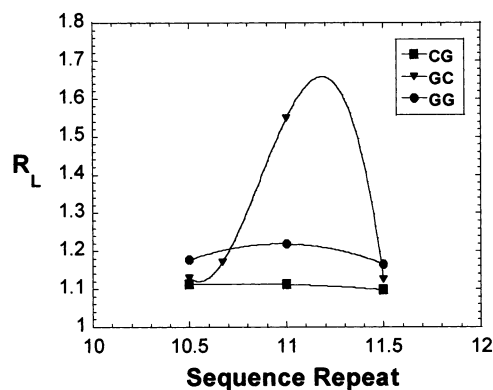


FIGURE 3:  $R_L$  values as a function of sequence repeat for multimers of chain length 150 bp for sequences of class I (G-tract only), having a sequence repeat of 21–23 bp (Table 2). The maximum of the graphs represents the apparent helical twist of that sequence, and the  $R_L$  value at that point represents the twist-independent curvature of the sequence.

reported to be the optimal helical repeat for this sequence motif (12).

The results (Figure 3, Table 2) show that sequences containing the GGGCCC motif, phased 11-bp apart, show appreciable bending. The bending at the maximum of the graph shown in Figure 3 has a  $R_L$  (150 bp) of 1.66, which corresponds to a bend angle of  $11.2^\circ$  per turn. The apparent helical repeat of these sequences is 11.2 bp/turn. Thus, the curvature in these sequences is 60% of the largest curvature observed to date in DNA sequences, that of phased  $A_6$ -tracts, and is currently the most bent sequence observed without adjacent A-tracts and without divalent ions. Previous studies on GGGCCC containing sequences have not observed such significant bending because they either used nonoptimal sequence repeats in the studied sequences (14) or used GC-tracts that are longer than half a helical turn (GGGCCCC, ref 12). As previously observed for bending associated with A-tracts, maximal bending is observed in sequences containing an  $A_6$ -tract. Bending magnitude is decreased in sequences containing an  $A_4$ -,  $A_5$ -, or  $A_7$ -tract (35).

Sequences containing the GGGGGG motif are only weakly bent. The  $R_L$  (150 bp) value at the maximum of the graph in Figure 3, 1.22, is just above the detection limit of the method (which is  $R_L = 1.2$ , ref 24) and corresponds to a bend angle of  $6.5^\circ$  per helical turn. The apparent helical repeat of these sequences is 11.1 bp/turn, in accord with previous studies (19). Sequences containing the CCCGGG motif are not bent at all, according to our results, or are only very weakly bent, below the detection limit of this method (which is around  $5^\circ$  per helical turn, ref 24).

**Extent of Influence of Nonadjacent G-Tracts on A-Tract Bending.** Brukner et al. (29) suggested, based on ligation-ladder analysis of the sequence AAAA ACTCTCTA AAAA- ACTCTCGGGCCCTAGAGGGCCCTAGA, that the bending of the GC step in the context of GGGCCC (in the absence of  $Mg^{2+}$  ions) is as high as that of the AA in the context of AAAAAA. This means that they apparently observed a full cancellation of AAAAAA bending by the GGGCCC-tract, when they were positioned one helical repeat apart. As discussed above, in our constructs (class IV, Table 1 and Figure 1D) the extent of modulation is much smaller. We suggest that the phenomenon that Brukner et al. (29) observed is due to loss of A-tract phasing in their sequence.

The nucleotide at the 3' end of this sequence is an A, which when ligated to form multimers adds to the A<sub>5</sub> motif at the 5' end of the sequence, thus creating an A<sub>6</sub>-tract. Hence, the spacing between the two A-tract centers is now 11.5 bp. At this phasing a substantial part of A-tract bending is canceled out (22, 35). The other part is canceled by the GGGCC-tract, as we observe. Thus, at present it seems that the maximal influence that a non-A-tract sequence element can exert on A-tracts is  $\pm 23\%$ .

*Do A-Tracts Influence the Structure of the Sequences Flanking Them or Are They Influenced by Them?* We have shown here and previously (22) that putting any DNA sequence between two phased A-tracts suppresses their intrinsic bending capabilities. We now show that these intrinsic bending properties will be expressed only when they are located five base pairs away from A-tracts. It has been proposed for several dinucleotides (36, 37) and longer tracts (14, 38) that they adopt a bistable conformation, which means that they adopt different conformations as a function of sequence context. We argue that all DNA sequences are bistable in their conformation when it comes to their interaction with phased A-tracts. However, some sequence motifs may be more bistable than others, and this will manifest itself in larger conformational differences between environments within and outside A-tract regions. It is surprising that sequences as diverse as CCCGGG and GGGCCC influence A-tract bending to similar degrees. The bent GGGCCC-tract influences A-tracts in the context of the GCPAA sequence (Figure 1C) to similar extent that the nonbent CCCGGG-tract influences A-tract bending in the CGABL sequence (Figure 1F), relative to the yardstick provided by the A<sub>6</sub>neut sequence. It may indicate that intrinsic bending is not the only cause for the observed variability in A-tract bending and/or that A-tracts influence the neighboring DNA sequences even when they are located five base pairs away from them (i.e., that net global bending is not additive even in these cases). Alternatively, CCCGGG may be the true neutral sequence, and A<sub>6</sub>neut is slightly bent into the major groove.

Hizver et al. (39) have recently solved the crystal structure of an oligomer containing the A-tract, AATT, which is intrinsically bent toward the minor groove at the center of the A-tract, in agreement with the findings of solution studies. In fact, according to this study (39) in all other crystal structures, containing an AATT-tract, there is a global bend directed toward the A-tract minor groove. However, in the other studies this bend was masked by another bend induced by crystal packing forces (39). Thus, A-tracts are not polymorphic in structure and are not influenced by sequence context or crystal packing forces. They are a dominant and invariable DNA sequence element, and their effect extends, or flows downstream into the sequences surrounding it on its 3'-side. Base pairs that are five base pairs downstream to A-tracts are still being affected by them, and the effect may extend even further. That the effect of A-tracts extends only into the 3' adjoining region can be explained by the nonuniformity of the minor groove width of A-tracts. Whereas the 5'-end of the minor groove is wide, at least as much as the average width of random sequence B-DNA, it is much narrower at the 3'-end (30–32) and approaches the width of poly (dA)•poly (dT) at tracts seven base pairs or longer (31). It takes about five base pairs into the adjoining

region for the minor groove to regain its normal width. If A-tracts are placed five base pairs apart (as in class II, Table 1), the sequence between them are all affected and do not have a chance of showing their true characteristic, regardless of their exact sequence.

## CONCLUSIONS

We have previously observed (22) that sequences immediately flanking A-tracts do modulate the extent of A-tract bending, but only by  $\pm 10\%$ . This observation remains valid. We now add that this is due to the rippling of the influence of A-tract structure into the 3'-flanking region, such that these regions do not show their true intrinsic properties. The intrinsic structural properties of any non-A-tract sequence are thus suppressed in the vicinity of the dominant A-tracts. When non-A-tract regions are removed by five base pairs from A-tracts, or are placed only at the 5' side of A-tracts, their true nature may be expressed but not necessarily its full extent. We observe here that the maximal influence of G-tracts on the magnitude of a combined A- and G-tract sequence is  $\pm 23\%$ . These sequence elements may not be the only ones capable of significantly modulating the extent of A-tract bending, nor are necessarily the best ones. A systematic search is presently conducted in our laboratory for such sequence motifs.

## ACKNOWLEDGMENT

The authors thank Drs. Donald Crothers and Zippi Shakked for helpful comments on the manuscript.

## REFERENCES

- Luisi, B. (1995) in *DNA-Protein: Structural interactions* (Lilley, D. M. J., Ed.) pp 1–48, IRL Press, Oxford.
- Travers, A. A. (1995) in *DNA-Protein: Structural interactions* (Lilley, D. M. J., Ed.) pp 49–75, IRL Press, Oxford.
- Dickerson, R. E. (1999) in *Oxford Handbook of Nucleic Acid Structure* (Neidle, S., Ed.) pp 145–197, Oxford University Press, Oxford.
- Crothers, D. M., Haran, T. E., and Nadeau, J. G. (1990) *J. Biol. Chem.* 265, 7093–7096.
- Crothers, D. M., and Shakked, Z. (1999) in *Oxford Handbook of Nucleic Acid Structure* (Neidle, S., Ed.) pp 455–470, Oxford University Press, Oxford.
- Marini, J. C., Levene, S. D., Crothers, D. M., and Englund, P. T. (1982) *Proc. Natl. Acad. Sci. U.S.A.* 79, 7664–7668.
- Wu, H.-M., and Crothers, D. M. (1984) *Nature* 308, 509–513.
- Beutel, B. A., and Gold, L. (1992) *J. Mol. Biol.* 228, 803–812.
- Nagaich, A. K., Bhattacharyya, D., Brahmachari, S. K., and Bansal, M. (1994) *J. Biol. Chem.* 269, 7824–7833.
- Widlund, H. R., Cao, H., Simonsson, S., Magnusson, E., Simonsson, T., Nielsen, P. E., Kahn, J. D., Crothers, D. M., and Kubista, M. (1997) *J. Mol. Biol.* 267, 807–17.
- Brukner, I., Jurukovski, V., Konstantinovic, M., and Savic, A. (1991) *Nucleic Acids Res.* 19, 3549–3551.
- Brukner, I., Susic, S., Dlakic, M., Savic, A., and Pongor, S. (1994) *J. Mol. Biol.* 236, 26–32.
- Dlakic, M., and Harrington, R. E. (1995) *J. Biol. Chem.* 270, 29945–29952.
- Dlakic, M., and Harrington, R. E. (1996) *Proc. Natl. Acad. Sci. U.S.A.* 93, 3847–3852.
- Brukner, I., Sanchez, R., Suck, D., and Pongor, S. (1995) *J. Biomol. Struct. Dyn.* 13, 309–317.
- De Santis, P., Palleschi, A., Savino, M., and Scipioni, A. (1990) *Biochemistry* 29, 9269–9273.
- Bolshoy, A., McNamara, P., Harrington, R. E., and Trifonov, E. N. (1991) *Proc. Natl. Acad. Sci. U.S.A.* 88, 2312–2316.
- Young, M. A., Ravishanker, G., Beveridge, D. L., and Berman, H. M. (1995) *Biophys. J.* 68, 2454–2468.

19. Biburger, M., Niederweis, M., and Hillen, W. (1994) *Nucleic Acids Res.* 22, 1562–1566.
20. Sambrook, J., Fritsch, E. F., and Maniatis, T. (1989) *Molecular cloning. A laboratory manual*, 2nd ed., Cold Spring Harbor Laboratory, Cold Spring Harbor, NY.
21. Haran, T. E., and Crothers, D. M. (1989) *Biochemistry* 28, 2763–2767.
22. Haran, T. E., Kahn, J. D., and Crothers, D. M. (1994) *J. Mol. Biol.* 244, 135–143.
23. Shatzky-Schwartz, M., Arbuckle, N. D., Eisenstein, M., Rabinovich, D., Bareket-Samish, A., Haran, T. E., Luisi, B. F., and Shakked, Z. (1997) *J. Mol. Biol.* 267, 595–623.
24. Koo, H. S., and Crothers, D. M. (1988) *Proc. Natl. Acad. Sci. U.S.A.* 85, 1763–1767.
25. Koo, H. S., Drak, J., Rice, J. A., and Crothers, D. M. (1990) *Biochemistry* 29, 4227–4234.
26. Peck, L. J., and Wang, J. C. (1981) *Nature* 292, 375–377.
27. Rhodes, D., and Klug, A. (1981) *Nature* 292, 376–378.
28. Brukner, I., Sanchez, R., Suck, D., and Pongor, S. (1995) *EMBO J.* 14, 1812–1818.
29. Brukner, I., Dlakic, M., Savic, A., Susic, S., Pongor, S., and Suck, D. (1993) *Nucleic Acids Res.* 21, 1025–1029.
30. Burkhoff, A. M., and Tullius, T. D. (1987) *Cell* 48, 935–943.
31. Nadeau, J. G., and Crothers, D. M. (1989) *Proc. Natl. Acad. Sci. U.S.A.* 86, 2622–2626.
32. MacDonald, D., Herbert, K., Zhang, X., Polgruto, T., and Lu, P. (2001) *J. Mol. Biol.* 306, 1081–1098.
33. Drak, J., and Crothers, D. M. (1991) *Proc. Natl. Acad. Sci. U.S.A.* 88, 3074–3078.
34. Saenger, W. (1984) *Principles of Nucleic Acid Structure*, Springer-Verlag, New York.
35. Koo, H. S., Wu, H. M., and Crothers, D. M. (1986) *Nature* 320, 501–506.
36. El Hassan, M. A., and Calladine, C. R. (1998) *J. Mol. Biol.* 282, 331–343.
37. El Hassan, M., and Calladine, C. R. (1997) *Philos. Trans. R. Soc. London, Ser. A* 355, 43–100.
38. Zhurkin, V. B., Gorin, A. A., Charakhchyan, A. A., and Ulyanov, N. B. (1990) in *Theoretical Biochemistry and Molecular Biophysics* (Beveridge, D. L., and Lavery, R., Eds.) pp 409–429, Adenine Press, Schenectady, NY.
39. Hizver, J., Rozenberg, H., Frolov, F., Rabinovich, D., and Shakked, Z. (2001) *Proc. Natl. Acad. Sci. U.S.A.* 98, 8490–8495.

BI020662W